Biochimica et Biophysica Acta 1797 (2010) 435–442

Contents lists available at ScienceDirect

Biochimica et Biophysica Acta

journal homepage: www.elsevier.com/locate/bbabio

Stimulation of F_1-ATPase activity by sodium dodecyl sulfate

Mohammad Delawar Hossain [a,b], Shou Furuike [a,1], Yasuhiro Onoue [a,c], Kengo Adachi [a,2], Masasuke Yoshida [d,e], Kazuhiko Kinosita Jr. [a,*]

[a] Department of Physics, Faculty of Science and Engineering, Waseda University, Shinjuku-ku, Tokyo 169-8555, Japan
[b] Department of Physics, School of Physical Sciences, Shahjalal University of Science and Technology, Sylhet-3114, Bangladesh
[c] Department of Functional Molecular Science, The Graduate University for Advanced Studies (Sokendai), Okazaki, Aichi 444-8585, Japan
[d] Chemical Resources Laboratory, Tokyo Institute of Technology, Nagatsuta 4259, Yokohama 226-8503, Japan
[e] ATP-Synthesis Regulation Project, International Cooperative Research Project (ICORP), Japan Science and Technology Agency (JST), Aomi 2-41, Tokyo 135-0064, Japan

ARTICLE INFO

Article history:
Received 3 August 2009
Received in revised form 1 December 2009
Accepted 24 December 2009
Available online 4 January 2010

Keywords:
Single molecule
Optical microscopy
Detergent
Torque
ATP synthase
ATP hydrolysis

ABSTRACT

F_1-ATPase is a rotary molecular motor in which the γ subunit rotates inside the cylinder made of $\alpha_3\beta_3$ subunits. We have studied the effects of sodium dodecyl sulfate (SDS) on the rotational and ATP hydrolysis activities of F_1-ATPase. Bulk hydrolysis activity at various SDS concentrations was examined at 2 mM ATP. Maximal stimulation was obtained at 0.003% (w/v) SDS, the initial (least inhibited) activity being about 1.4 times and the steady-state activity 3–4 times the values in the absence of SDS. Rotation rates observed with a 40-nm gold bead or a 0.29-μm bead duplex as well as the torque were unaffected by the presence of 0.003% SDS. The fraction of beads that rotated, in contrast, tended to increase in the presence of SDS. SDS seems to bring inactive F_1 molecules into an active form but it does not alter or enhance the function of already active F_1 molecules significantly.

1. Introduction

ATP synthase catalyzes the synthesis of ATP from ADP and inorganic phosphate (Pi) in bacteria, animals and plants by oxidative phosphorylation or photophosphorylation processes [1–4]. The ATP synthase is a reversible molecular machine that consists of a membrane-embedded proton-conducting portion F_o and a protruding portion F_1 in which ATP is synthesized or hydrolyzed. Boyer [5] and Oosawa [6] proposed that both F_o and F_1 are rotary motors and that the two motors are coupled by a common rotary shaft. The proton flow through F_o rotates the shaft, which in turn induces conformational changes in F_1 that results in ATP synthesis; whereas ATP hydrolysis in F_1 causes reverse rotation of the shaft that forces protons to flow in the reverse direction. Isolated F_1 only hydrolyzes ATP and is called F_1-ATPase. The minimal ATPase-active subcomplex of F_1 consists of $\alpha_3\beta_3\gamma$ subunits which we call as F_1 in this article. According to a crystal structure [7] of F_1, a central γ subunit is surrounded by an $\alpha_3\beta_3$ cylinder where three α and three β subunits are arranged alternately. The three catalytic β subunits in the structure bound (an analog of) ATP, ADP and none, whereas the three non-catalytic α subunits bound only (the analog of) ATP.

Rotation of the central γ subunit inside the $\alpha_3\beta_3$ cylinder occurs in 120° steps each driven by hydrolysis of one ATP molecule [8]. The 120° step is resolved into 80–90° and 40–30° substeps, and ATP is hydrolyzed during the short (~ms) dwell at 80–90° [8–10]. The 80–90° substep is driven by ATP binding and ADP release, and the 40–30° substep by Pi release [11]. The F_1 is a reversible molecular machine in that reverse rotation of γ by an external force results in ATP synthesis [12,13]. The reversal of chemical reaction (ATP hydrolysis) by manipulation of the γ-angle alone implies a γ-dictator mechanism, in which the orientation of the γ-rotor relative to the $\alpha_3\beta_3$ stator determines which of the chemical reactions (binding/release of ADP, Pi and ATP, and synthesis/hydrolysis of ATP) is to occur in each catalytic site.

The activity of F_1 is affected by various detergents [14–17]. An example is lauryldimethylamine oxide (LDAO) that stimulates the steady-state activity of thermophilic F_1 (TF_1) fourfold by rescuing inhibited F_1 [14]. Sodium dodecyl sulfate (SDS) is a detergent commonly used as a denaturant. Under certain conditions, however, SDS has been shown to activate/stimulate some protein enzymes [18–20]. In this article we studied the effect of SDS on the hydrolysis and rotation activities of F_1. We found that, at very low concentrations, SDS also stimulates F_1.

* Corresponding author. Department of Physics, Faculty of Science and Engineering, Waseda University, 3-4-1 Okubo, Shinjuku-ku, Tokyo 169-8555, Japan. Tel.: +81 3 5952 5871; fax: +81 3 5952 5877.
E-mail address: kazuhiko@waseda.jp (K. Kinosita).
[1] Current addresses: Department of Physics, Osaka Medical College, Daigaku-machi 2-7, Takatsuki City, Osaka 569-8686, Japan.
[2] Current addresses: Department of Physics, Gakushuin University, Toshima-ku, Tokyo 171-8588, Japan.

0005-2728/$ – see front matter © 2009 Elsevier B.V. All rights reserved.
doi:10.1016/j.bbabio.2009.12.018

2. Materials and methods

2.1. Materials

SDS was purchased from Bio-RAD Laboratories (Hercules, CA). ADP, ATP (Roche Diagnostics, Mannheim, Germany), BSA and phosphoenolpyruvate were from Sigma-Aldrich (St. Louis, MO). In rotation or ATP hydrolysis activity measurements, $[Mg^{2+}]$ always exceeded by 2 mM over [ATP]s.

2.2. Purification and biotinylation of F_1

A mutant (α-C193S, β-His_{10} at amino terminus, γ-S107C, γ-I210C) $\alpha_3\beta_3\gamma$ subcomplex derived from a thermophilic *Bacillus* PS3 was purified as described [21,22] with some modifications. The *E. coli* cell lysate was heat treated at 65 °C for 8–10 min in a hot water tank. F_1 purified with a Ni^{2+}-nitrilotriacetic acid (Ni-NTA) Superflow column (Qiagen, Hilden, Germany) was passed through a butyl-Toyopearl column (650 M, Tosoh, Tokyo, Japan) to remove endogenously bound nucleotide by washing with 40 column volumes (400 ml) of buffer A (100 mM potassium phosphate, pH 7.0, and 2 mM EDTA) containing 10% saturated ammonium sulfate. Eluent at 1–0% ammonium sulfate was precipitated in buffer A containing 70% ammonium sulfate and 2 mM dithiothreitol (DTT) and stored at 4 °C. Before use, the precipitate was dissolved in buffer A and passed through a size exclusion column (Superdex 200, 10/300 GL, GE Healthcare UK Ltd., UK) pre-equilibrated with buffer A to remove DTT and possible denatured enzyme. The amount of nucleotide that remained was estimated on a reverse-phase column (TSK-GEL ODS-80Ts, Tosoh) equilibrated with 100 mM sodium phosphate, pH 6.8 [23].

Purified F_1 was biotinylated at the two cysteines (γ-107C and γ-210C) by incubation with fourfold molar excess of 6-{*N*′-[2-(*N*-maleimide)ethyl]-*N*-piperazinylamide}hexyl-D-biotinamide (Dojindo, Kumamoto, Japan) for 30 min at room temperature. A size exclusion column (Superdex 200, 10/300 GL) pre-equilibrated with buffer A was used to remove unbound biotin. Biotinylated F_1 was frozen with liquid nitrogen and stored at −80 °C.

2.3. Measurement of hydrolysis activity of F_1

A spectrophotometer (U-3300, Hitachi, Japan) equipped with a thermostat was used to measure the ATP hydrolysis activity of F_1. An ATP regenerating system that contained, in buffer B (10 mM Mops-KOH pH 7.0, 50 mM KCl and 2 mM $MgCl_2$), 0.2 mM NADH, 1 mM phosphoenolpyruvate, 250 μg ml^{-1} pyruvate kinase (rabbit muscle, solution in glycerol, Roche Diagnostics, Mannheim, Germany) and 50 μg ml^{-1} lactate dehydrogenase (hog muscle, Roche) was made prior to activity measurement. 1.8–1.9 ml of the ATP regenerating solution was poured into a quartz cuvette fitted in the holder of the spectrophotometer and a desired amount of SDS was also added. Then MgATP was rapidly mixed. The reaction was started by the addition of F_1 to a final concentration of 5–10 nM. The measurement was carried out at 23 °C and hydrolysis rate was determined from the absorbance decrease of NADH at 340 nm [24].

2.4. Making Ni-NTA glass surface

Glass surfaces were functionalized with Ni-NTA to immobilize F_1. Glass coverslips (NEO Micro Cover Glass, No.1, 24×32 mm^2, Matsunami, Osaka, Japan) placed on a ceramic glass holder were immersed in 12 N KOH for 24 h and then vigorously washed with ultra pure water [12]. The washed coverslips were treated in a solution containing 0.02% (v/v) acetic acid and about 2% (v/v) 3-mercaptopropyltrimethoxysilane (TSL8380, Toshiba GE silicone, Tokyo, Japan) with continuous stirring at 60 °C in a fume hood for 15–20 min. The coverslips were treated in the same silane solution for further 2 h at 90 °C in a constant-temperature oven. The coverslips were cooled to room temperature and washed with ultra pure water. Further treatments below were all at room temperature. 100 mM DTT in 10 mM Mops-KOH, pH 7.0 was sandwiched between pairs of coverslips and left for 20 min to reduce the –SH groups of the silane on the glass surfaces. Following washing in ultra pure water, the coverslips were again paired to sandwich 10 mg ml^{-1} Maleimide-C_3-NTA (Dojindo) in 10 mM Mops-KOH, pH 7.0 for 30 min. After washing, the coverslips were reacted with 10 mM $NiCl_2$ for 20 min. Finally, the coverslips were washed and stored in ultra pure water and used within a few weeks.

2.5. Observation of rotation of F_1 with polystyrene beads

A flow chamber for microscopic observation was constructed of a Ni-NTA coated bottom coverslip (24×32 mm^2) and a top uncoated coverslip (18×18 mm^2) separated by two greased strips of Parafilm cover sheet. An ATP regenerating system consisting of buffer B with 0.2 mg ml^{-1} creatine kinase (rabbit muscle, Roche) and 2.5 mM creatine phosphate (Roche) was made. One chamber volume of 0.5–1 nM biotinylated F_1 in buffer B was infused in the chamber and incubated at room temperature for 2 min to fix F_1 on the Ni-NTA coated

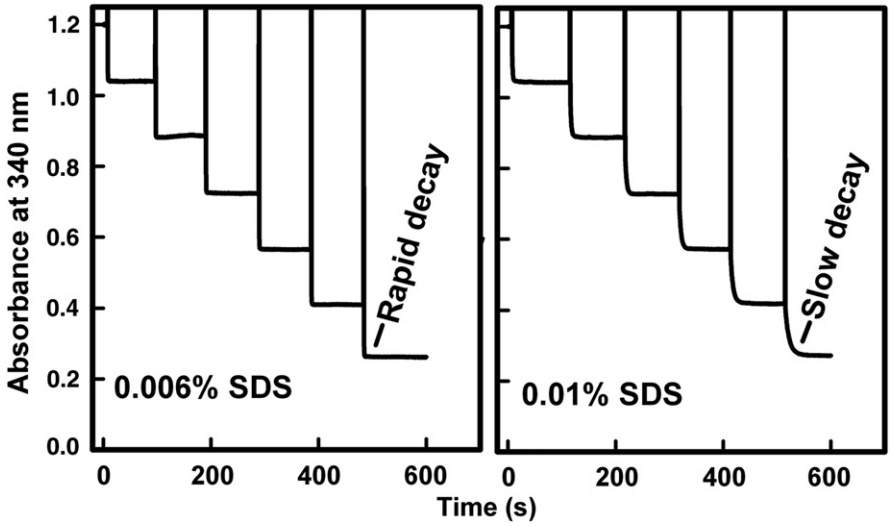

Fig. 1. Stability of the ATP regenerating system checked by adding ADP as substrate and following the decrease in the NADH absorbance at 340 nm.

glass surface through the histidine tags. Unbound F_1 was removed by washing with BSA (5 mg ml^{-1}) in buffer B. Streptavidin coated beads of diameter 0.29 μm (Seradyn, Indianapolis, IN) were washed and adjusted to a final concentration of 0.1% (w/v) in 5 mg ml^{-1} BSA. One chamber volume of the beads was infused into the chamber and kept for 15 min at room temperature to let them attach to the biotinylated γ subunit of the $\alpha_3\beta_3\gamma$ complex. The flow cell was washed three times with buffer B to remove unbound beads. Finally, five chamber volumes of the regenerating system above containing desired amounts of MgATP and SDS were infused and the chamber was sealed with silicon grease to avoid evaporation. Rotation was observed at 23 °C on an inverted microscope (IX71, Olympus, Tokyo, Japan) with a stable mechanical stage (KS-O, ChuukoushaSeisakujo, Tokyo, Japan). Bead images were captured with a CCD camera (Lynx IPX-VGA210L, Imperx, Boca Raton, FL) at 500 frames s^{-1} as an 8-bit AVI file. Centroid of the bead images was calculated as described [8]. A duplex of beads was always selected for analysis.

2.6. Observation of rotation with gold beads

The surfaces of 40-nm gold beads (EM.GC40, a suspension at 9×10^{10} particles ml^{-1}, BBInternational, Cardiff, UK) were functionalized with thiolated streptavidin and thiolated polyethylene glycol (PEG) as follows. To 5 mg ml^{-1} streptavidin (Thermo Fisher Scientific, Rockford) in buffer C (10 mM Mops-KOH, pH 7.0, 50 mM KCl) containing 10 mM Bond-Breaker TCEP Solution (Thermo Fisher Scientific), 1/50 volume of 25 mM dithiobis(succinimidylpropionate) (Thermo Fisher Scientific) in dimethyl sulfoxide was added and incubated for 1 h at room temperature. Thiolated PEG was prepared by mixing equal volumes of 40 mM NHS-mdPEG (molecular weight: 1214, Quanta BioDesign, Powell) in dimethyl sulfoxide and 2 mM 2-aminoethanethiol (Tokyo Chemical Industry, Tokyo) in buffer C containing 10 mM Bond-Breaker TCEP Solution, and letting the reaction proceed at room temperature for >1 day. To the gold bead suspension, 1/100 volume each of the thiolated streptavidin solution and the thiolated PEG solution were added in rapid succession and stored at 4 °C for >1 day. The beads were used within a few weeks. Before use, we washed the gold beads extensively with buffer C to remove free streptavidin.

Biotinylated F_1 (100–500 pM) in buffer C was infused into an observation chamber made of Ni-NTA coated bottom and uncoated top coverslips [22]. After washing out unbound F_1 with buffer C, we infused 10 mg ml^{-1} BSA in buffer C to prevent nonspecific binding. After extensive washing with buffer C, we infused the modified gold beads and washed away excess beads with buffer C. Finally, we infused buffer C containing 2 mM MgATP, 2 mM $MgCl_2$, and an ATP regenerating system (0.2 mg ml^{-1} creatine kinase and 2.5 mM creatine phosphate).

Bead rotation was observed at 23 °C by laser dark-field microscopy [8] on an inverted microscope (Olympus IX70) with some modifications (S. Furuike, unpublished): instead of the oblique illumination [8], we illuminated the sample along the optical axis with a parallel beam of diameter ~10 μm and power <10 mW, by collimating a laser beam (Millennia IIs, Spectra-Physics) with an objective placed above the sample. After the sample, the transmitted beam was let out through a pinhole in a mirror while the mirror deflected the scattered light to form a dark-field image of the beads. Images were captured with a high-speed CMOS camera (FASTCAM-DJV, Photron, Tokyo) at 8000 frames s^{-1} as an 8-bit AVI file. Centroid of bead images was calculated as described [8].

3. Results

3.1. Stability of ATP regenerating system

The stability of the ATP regenerating system used for the hydrolysis assay was checked against SDS for 10 min. At 0.01% SDS, the absorbance decay following ADP addition became progressively slower, indicating gradual deterioration of the regeneration system by SDS (Fig. 1). In contrast, the decay remained rapid to at least ~500 s below this SDS concentration. The hydrolysis activity of F_1 was examined at ≤0.006% SDS.

3.2. SDS dependence of the hydrolysis activity

The response of F_1 to SDS was examined by measuring the ATPase activity of F_1 in the presence of increasing concentrations of SDS (0–0.006%) at 2 mM ATP (Fig. 2). The F_1 activity was stimulated with the increase of SDS concentration and reached a maximal value at 0.003% of SDS (Fig. 2B). At higher SDS concentrations the activity started to decrease again. In these high concentrations, SDS likely destabilizes F_1. Maximal stimulation of the initial activity, estimated over 2–7 s after the start of F_1 addition (yellow lines in Fig. 2A), was about 1.4 fold at 0.003% SDS.

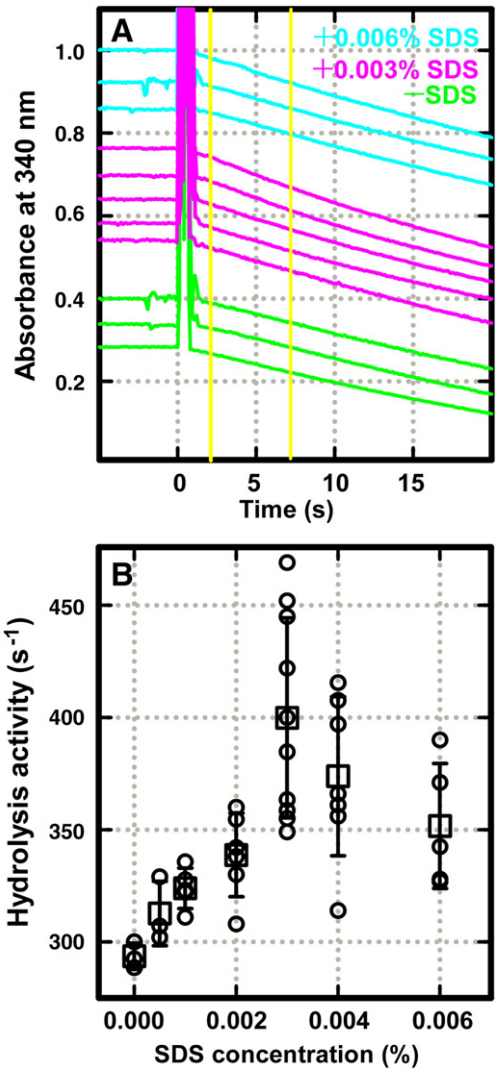

Fig. 2. (A) Representative time courses of hydrolysis activity at 2 mM ATP in the presence and absence of SDS. The yellow vertical lines show the region (between 2 and 7 s after the F_1 addition at 0 s) where we estimated the initial activity. (B) Response of ATPase activity of F_1 to increasing concentrations of SDS. The activity was measured at 2 mM ATP which was saturating and at a constant concentration of F_1 (5 nM). Small circles show individual measurements, and squares are their averages with the error bars showing the standard deviations.

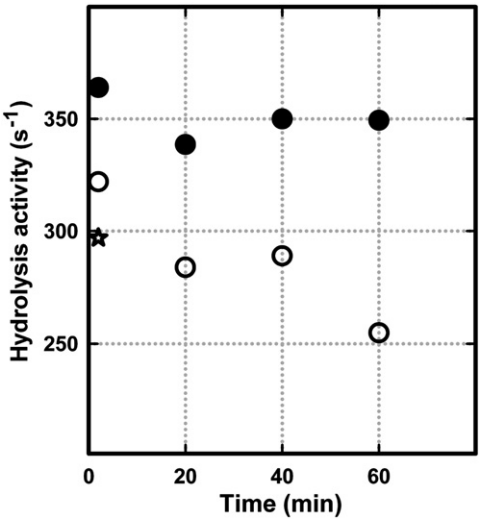

Fig. 3. The initial hydrolysis activity at 2 mM ATP after pre-incubation with 0.003% SDS. At indicated times during incubation, an aliquot was drawn and subjected to the activity assay with (closed circles) or without (open circles) 0.003% SDS in the assay medium. The star indicates the activity of the control without SDS pre-incubation and without SDS in the assay medium.

3.3. Hydrolysis activity after pre-incubation with SDS

To see whether the stimulatory effect of SDS is persistent or of a transient nature possibly followed by a slow deactivation (as for the regenerating system in Fig. 1), we pre-incubated 1 μM F_1 with 0.003% SDS. At intervals we took an aliquot and measured the hydrolysis activity in the ATP regenerating system with or without SDS (Fig. 3). When monitored in the presence of SDS (closed circles), the activity remained constant over the pre-incubation period of 60 min, showing that 0.003% SDS does not deteriorate F_1 at least for 1 h, and that the stimulation by SDS is instantaneous and not cumulative. When hydrolysis was assayed in the absence of SDS, on the other hand, pre-incubation with SDS failed to show stimulative effects (open circles). SDS exerts its effect only while it is present. The open circles show some decline with time, but we are not sure if this trend is significant.

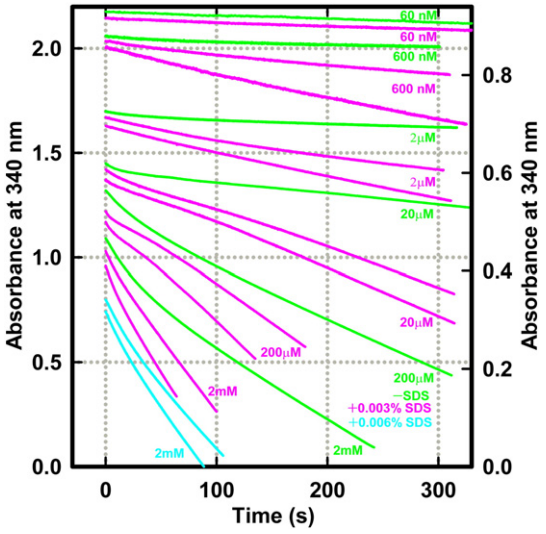

Fig. 4. Time courses of ATP hydrolysis by F_1 at different [ATP]s in the presence or absence of SDS. Cyan, 0.006% SDS; pink, 0.003% SDS; green, no SDS (data from [22]). Because the results were variable in the presence of SDS, the fastest and slowest time courses are shown for each [ATP] (except at 60 nM). The right-hand axis applies to the activities at 600 nM and below. [F_1] was 5 nM except at 60 nM ATP where [F_1] was 10 nM.

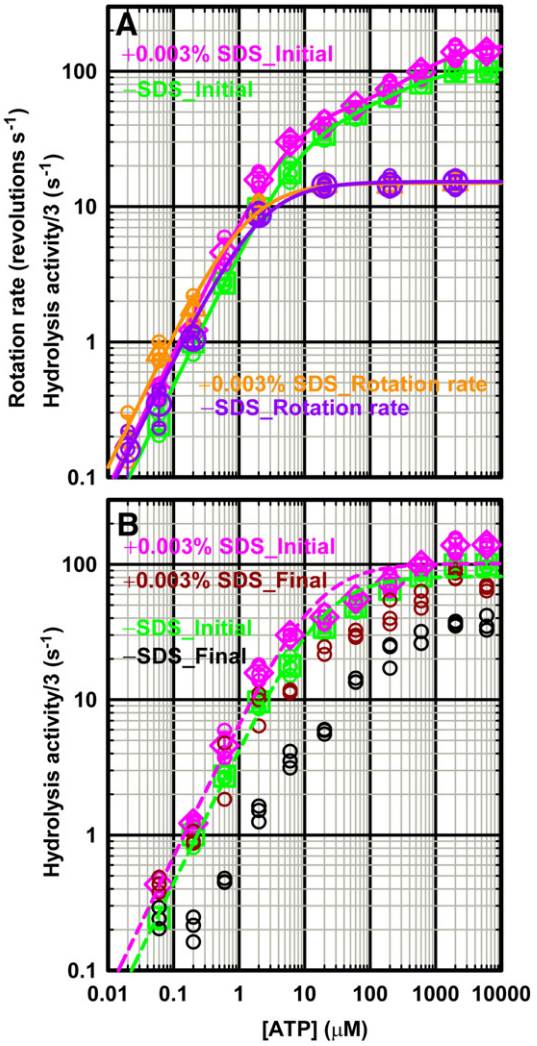

Fig. 5. Comparison of hydrolysis and rotation rates in the presence and absence of SDS. (A) Comparison between the initial hydrolysis rates and rotation rates. (B) Initial and final (steady-state) hydrolysis activities. For hydrolysis in (A) and (B), the rates are divided by three for comparison with the rotation rates. Pink and dark red circles are the initial and steady-state hydrolysis rates measured in the presence of 0.003% SDS. Pink diamonds show the averages of initial rates. Green and black circles are the initial and steady hydrolysis rates measured in the absence of SDS, green squares showing the averages (data from [22]). The initial hydrolysis activity was estimated at 2–7 s after the addition of nucleotide-free F_1 (2 μM ATP and above for ± SDS), 2–15 s (600 and 200 nM ATP without SDS), 2–17 s (600 nM ATP with SDS), 3–33 s (200 nM ATP with SDS), and for a ~300-s portion (60 nM ATP for ± SDS). Values at 60 nM ATP have been corrected for a small decline in the absorbance observed in the absence of F_1. The steady-state hydrolysis activities were estimated from the final 60-s portion of a time course in the absence of SDS. In the presence of SDS, the steady-state activity was estimated from the final 20 s at 200 μM ATP and above, and 50 s at 60 μM to 200 nM ATP. Steady-state values were not estimated at 60 nM ATP. Dashed curves in (B) are fit with Michaelis–Menten kinetics, $V = V_{max}[ATP]/(K_m + [ATP])$, where V_{max} (without division by three) and K_m are 240 s^{-1} and 18 μM without SDS (green), and 300 s^{-1} and 15 μM with SDS (pink). Solid curves for hydrolysis in (A) are fit with two K_m values, $V = (V_{max1}K_{m2}[ATP] + V_{max2}[ATP]^2)/([ATP]^2 + K_{m2}[ATP] + K_{m1}K_{m2})$, where $V_{max1} = 150\ s^{-1}$, $K_{m1} = 10$ μM, $V_{max2} = 320\ s^{-1}$, and $K_{m2} = 400$ μM for hydrolysis without SDS (green) and $V_{max1} = 170\ s^{-1}$, $K_{m1} = 6.7$ μM, $V_{max2} = 480\ s^{-1}$, and $K_{m2} = 800$ μM with SDS (pink). Rotation rates in the presence (orange) and absence (violet) of SDS in (A) were estimated over >100 consecutive revolutions. The rotation rates saturated because of the hydrodynamic friction against the rotating beads [8]. Solid curves are fit with Michaelis–Menten equation, from which the apparent rate of ATP binding, k_{on}^{ATP}, was obtained as $3 \times v_{max}/K_m$. The rate was $2.3 \times 10^7\ M^{-1}\ s^{-1}$ ($v_{max} = 15.3$ revolutions s^{-1}) without SDS (violet) and $3.6 \times 10^7\ M^{-1}\ s^{-1}$ ($v_{max} = 14.9$ revolutions s^{-1}) with 0.003% SDS.

3.4. ATP dependence of hydrolysis activity in the presence of SDS

Activity measurements were carried out for 6 min in the absence or presence of 0.003% SDS at 23 °C. Starting from 2 mM ATP down to 60 nM, F_1 showed a biphasic time course in the absence of SDS (green lines in Fig. 4): an initial burst rapidly decelerated into a steady final state (at 60 nM the activity was too low for the distinction). When nucleotide-free F_1 is added to start the reaction, it hydrolyzes ATP rapidly. As time passes a portion of the enzyme is inhibited by tightly binding MgADP and the inhibited fraction accumulates gradually until a steady state is reached that represents a dynamic equilibrium between active and MgADP-inhibited forms [25]. At intermediate ATP concentrations some reactivation precedes the final steady state (the slight acceleration seen in the final portion of the green line at 20 μM ATP in Fig. 4), due to slow binding of ATP to non-catalytic sites which tends to rescue the enzyme from inhibition [26].

SDS at 0.003% increased both the initial and steady-state activities at all ATP concentrations (except possibly for 60 nM ATP where the effect was not clear). The stimulatory effect was more pronounced at the steady state than at the beginning. At intermediate ATP concentrations, SDS produced a marked triphasic behavior, where the initial burst was followed by a conspicuous lag before a rapid final phase set in. It appears as if SDS accelerates all reactions, the uninhibited initial hydrolysis, deceleration due to MgADP inhibition, and reactivation by ATP binding to non-catalytic sites.

One third of the ATP hydrolysis rates are plotted in Fig. 5 (for comparison with rotation rates described below). Both in the presence and absence of SDS the initial hydrolysis rates could not be fitted with a simple Michaelis–Menten kinetics, as has been shown in the absence of SDS [8]. If phosphate is removed from the medium completely, a Michaelis–Menten kinetics with a lower rate at saturating [ATP] would be obtained at least in the absence of SDS (R. Shimo-Kon, unpublished). The simple kinetics is also obtained in the presence of LDAO [8] which is a suppressor of MgADP inhibition [14–16].

3.5. Rotation of F_1 with a polystyrene bead duplex

Rotation of individual F_1 molecules was observed by attaching a 0.29-μm bead duplex to the γ subunit. Those bead duplexes that were attached obliquely against the glass surface, as judged by eye, were selected for the analysis of rotational motions to minimize the effects of surface obstruction. Rotation time courses at 2 mM and 200 nM ATP observed with or without SDS are shown in Fig. 6. At 2 mM ATP the rotation was basically smooth, except for occasional long pauses due

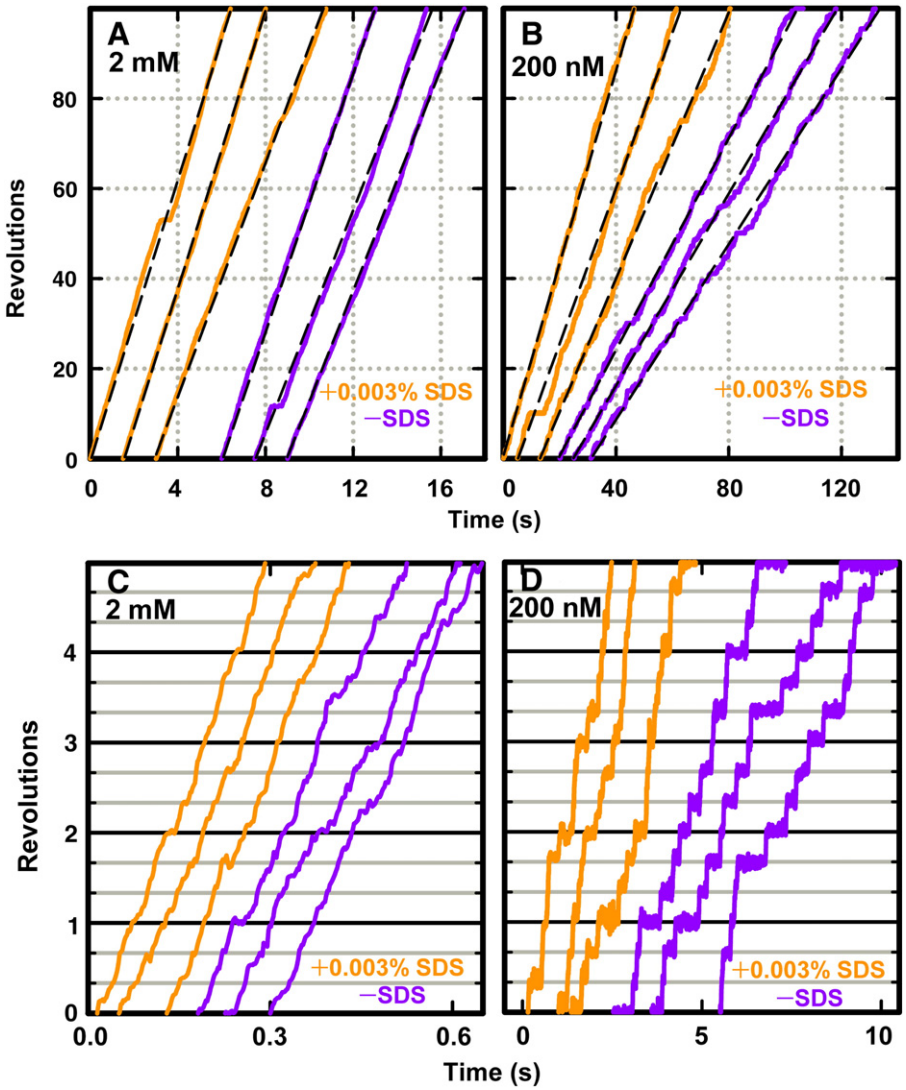

Fig. 6. Time courses of rotation of 0.29-μm bead duplexes at 2 mM and 200 nM ATP in the presence and absence of SDS. The broken black lines on the time courses (A and B) show the average rotation speeds over at least 100 revolutions. Magnified time courses (C and D) show short pauses (stumbling) and ATP-waiting dwells during rotation.

to MgADP inhibition. The rotary speed at 2 mM ATP, limited by the viscous friction against the bead duplex, appears unchanged in the presence of 0.003% SDS. At 200 nM ATP, rotation proceeded in steps of 120°, due to infrequent binding of ATP. At this [ATP] the average rotary speed was apparently higher in the presence of SDS. As seen in Fig. 6D, the dwells at 200 nM ATP tended to be shorter in the presence of SDS, accounting in part for the difference in the average rotary speed. The rotation at 2 mM ATP was also smoother in the presence of SDS (Fig. 6C), suggesting that SDS may somehow reduce surface obstructions.

Time-averaged rotary speeds for >100 consecutive revolutions uninterrupted by the MgADP inhibition are plotted against [ATP] in Fig. 5A. The apparent saturation above 2 μM ATP is due to the viscous friction: the torque F_1 produces is balanced by the frictional force on the bead duplex, and thus F_1 cannot rotate faster. The fact that the speed at saturation was the same whether 0.003% SDS was present or not implies that SDS does not affect the torque of F_1. The torque at 200 nM ATP, estimated from the rotary speed in each 120° stepping [22], was also insensitive to the presence of SDS (not shown).

Below 2 μM ATP where ATP binding was rate limiting, the time-averaged rotary speed was ~50% higher in the presence of 0.003% SDS. The apparent rate of ATP binding, calculated from the violet and orange fitting curves in Fig. 5A, was $2.3\times10^7\ M^{-1}\ s^{-1}$ without SDS (violet) and $3.6\times10^7\ M^{-1}\ s^{-1}$ with 0.003% SDS (orange). As discussed above, the difference may in part be due to reduction of surface obstruction by SDS. However, the binding rate estimated from the hydrolysis activity at low [ATP]s, $3V_{max1}/K_{m1}$, also showed a similar trend: $1.5\times10^7\ M^{-1}\ s^{-1}$ without SDS (green curve in Fig. 5A) and $2.5\times10^7\ M^{-1}\ s^{-1}$ with 0.003% SDS (pink). SDS may facilitate ATP binding to some extent, which could also explain the higher hydrolysis activity at saturating [ATP] (Fig. 2).

The most conspicuous effect of SDS on rotation was an increase in the number of rotating beads on the glass surface. Typically we observed a few rotating bead duplexes in a field of view of $47\times36\ \mu m^2$ (Fig. 7, Tables 1 and 2). Some bead duplexes exhibited random fluctuations and others were stuck on the glass surface. Presumably part of the most abundant single beads also rotated, but discerning rotation of the small (0.29 μm) beads was difficult. 0.003% SDS increased the fraction of rotating duplexes from 2.2% to 4.8% at 2 mM ATP (Table 1) and from 2.0% to 6.9% at 200 nM ATP (Table 2). Part of the increase might be ascribed to the fact that SDS tended to decrease the total number of beads on the surface (by 46% at 2 mM ATP and by 25% at 200 nM ATP for the chambers examined). But the two to threefold increases in the rotating fraction at high and low [ATP]s are largely consistent with the SDS-induced increase in the steady-state hydrolysis activity in Fig. 5B.

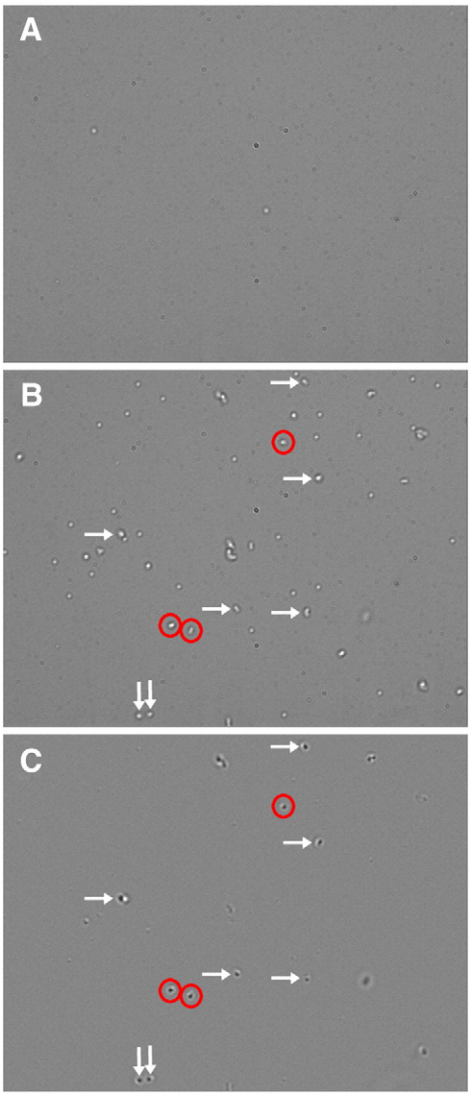

Fig. 7. Typical images of 0.29-μm polystyrene beads in the field of view $47\times36\ \mu m^2$. (A) Beads (white) non-specifically bound to the surface in the absence of F_1. Dark spots are dirt on the optical elements. (B) A snapshot of beads attached to F_1 at 200 nM ATP and 0.003% SDS. Red circles, rotating duplexes; white arrows, fluctuating duplexes. Others are duplexes stuck on the surface, or higher aggregates (three or more beads) and single beads of which some are moving. (C) Moving beads in (B). Images over a 10-s period starting with (B) were averaged, from which image (B) was subtracted, and then a constant was added to the difference image to set the zero level (no difference) gray. In (C), bead positions different from (B) appear white, while the original positions in (B) appear black. Unmarked objects in (C) are higher aggregates or single beads that moved, or beads that disappeared during the averaging period.

3.6. Rotation of F_1 with a 40-nm gold bead

Unloaded rotation of F_1 was observed by attaching a 40-nm gold bead(s) to the γ subunit. Time-averaged rotary speeds over consecutive 100 revolutions at 2 mM ATP are shown in Fig. 8. The speed varied considerably from bead to bead. On the average, we did not see significant increase in the rotary speed at 0.003% SDS, in contrast to the notable increase in the hydrolysis activity (Fig. 2B). We did not attempt extensive analyses of the number of rotating beads, but the trend was similar to the case of polystyrene beads above. A pair of observation chambers with and without SDS were compared on the same day: at 2 mM ATP, 95 rotating beads were found out of total 677 beads (14%) with 0.003% SDS, and 78 rotated of the total of 801 (9.7%) without SDS, each in 12 fields of view ($7.1\times7.1\ \mu m^2$); at 20 nM ATP, 62 rotated of 322 (19.3%) with SDS and 19 rotated of 465 (4.1%) without SDS, each in 8 fields. The implication is that SDS activates inactive or dormant F_1 rather than enhances the activity (rotary speed) of already active F_1. Beyond 0.01% SDS, both the speed and the number of rotating beads decreased, and the decrease became more severe with time (Fig. 8, crosses).

4. Discussion

The effects of an anionic detergent SDS on the hydrolysis and rotational activities of F_1 are presented in this report. Within the limit of the ATP regenerating system (≤0.006% SDS), SDS stimulates the ATP hydrolysis activity of F_1. The maximal stimulating SDS concentration is 0.003% (w/v) or ~100 μM, far below the critical micelle concentration of ~8 mM in water or ~3 mM at a higher ionic strength [27]. Binding of monomeric SDS somehow stimulates F_1, and the F_1–SDS complex is in equilibrium with the medium SDS because SDS must be present in the medium to exert its effect. A moderate (10–

Table 1
Summary of rotation data for 0.29-μm beads at 2 mM ATP in the absence and presence of 0.003% SDS.

	Number of rotating duplexes	Number of fluctuating duplexes	Number of duplexes stuck	Number of higher aggregates	Number of single beads	Total
−SDS						
Cell 1	21	130	109	124	727	1111
Cell 2	11	82	80	106	610	889
Cell 3	9	37	31	17	121	215
Cell 4	21	133	71	103	489	817
Cell 5	20	96	84	127	446	773
Average	16.4	95.6	75	95.4	478.6	761.0
SD	5.9	39.4	28.3	45.1	228.0	331.8
% Total	2.2	12.6	9.9	12.5	62.9	100
+SDS						
Cell 1	15	56	29	57	211	368
Cell 2	28	37	61	86	307	519
Cell 3	13	20	16	18	86	153
Cell 4	18	82	36	61	305	502
Cell 5	25	57	36	65	327	510
Average	19.8	50.4	35.6	57.4	247.2	410.4
SD	6.5	23.3	16.4	24.7	100.7	156.7
% Total	4.8	12.3	8.7	14.0	60.3	100

The numbers for each cell (observation chamber) are the sums over randomly selected ten fields of view ($47\times36\ \mu m^2$) each observed for 17 s at 2 mM ATP and 1 min at 200 nM ATP. Some beads stopped or started rotation during the observation period, and these were counted as rotating. The duplexes in the second to fourth columns may include some higher aggregates (three or more beads) that were not readily distinguishable from true duplexes. Higher aggregates and singles were counted as such irrespective of whether moving or not. Without F_1, the average number of beads per cell (ten fields of view) was 18.

20%) increase in the amylase activity has been observed at the SDS concentration of around 50 μM [18]. Activation of latent proteasome apparently requires an order of magnitude higher SDS concentration [19], which might be due to a higher protein concentration of 0.5 mg ml^{-1} employed in the study.

For our thermophilic F_1 (TF_1), the maximal stimulation by SDS is about 1.4-fold for the initial hydrolysis activity and the steady-state stimulation is three to fourfold (Figs. 4 and 5). At the steady state, much of F_1 is in the MgADP-inhibited state, and thus the major effect of SDS is to rescue F_1 from the inhibition. The neutral detergent LDAO also

Table 2
Summary of rotation data for 0.29-μm beads at 200 nM ATP in the absence and presence of 0.003% SDS.

	Number of rotating duplexes	Number of fluctuating duplexes	Number of duplexes stuck	Number of higher aggregates	Number of single beads	Total
−SDS						
Cell 1	8	64	28	31	308	439
Cell 2	9	95	69	94	332	599
Cell 3	9	91	87	77	292	556
Cell 4	11	89	39	58	259	456
Cell 5	11	82	37	49	211	390
Average	9.6	84.2	52	61.8	280.4	488
SD	1.3	12.2	24.9	24.5	47.0	86.6
% Total	2.0	17.3	10.7	12.7	57.5	100
+SDS						
Cell 1	38	59	63	56	272	488
Cell 2	20	55	24	46	173	318
Cell 3	10	52	24	31	102	219
Cell 4	35	99	64	39	267	504
Cell 5	23	58	22	34	164	301
Average	25.2	64.6	39.4	41.2	195.6	366.0
SD	11.4	19.4	22.0	10.0	72.8	124.6
% Total	6.9	17.7	10.8	11.3	53.4	100

See Table 1 for details.

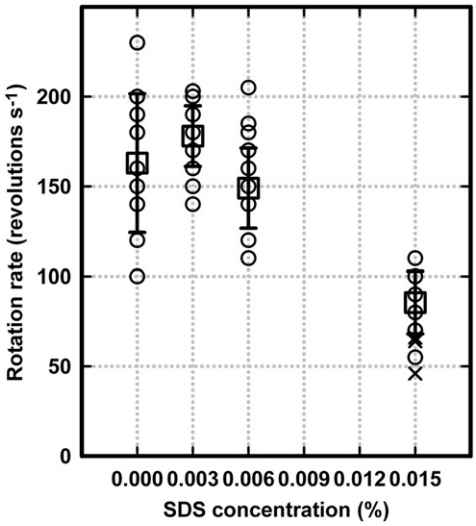

Fig. 8. Rotation of 40-nm gold beads attached to F_1, observed under a dark-field microscope, at various SDS concentrations and at 2 mM ATP in the presence of an ATP regenerating system. Small circles are rotary speeds of individual F_1 molecules, estimated over >100 revolutions, and large squares are their averages with error bars showing standard deviations. Crosses at 0.015% SDS show measurements after 1 h.

enhances the steady-state activity of TF_1 up to fourfold by promoting the release of MgADP tightly entrapped in a catalytic site [14]. SDS appears more effective, in the sense that 0.1% LDAO, compared to 0.003% SDS, is required for maximal stimulation. The rescue from the inhibition is consistent with the microscopic observation that the fraction of rotating beads, whether 0.29-μm polystyrene or 40-nm gold, increases in the presence of 0.003% SDS, although the analyses are not highly reliable because the rotating fraction was small. For population analyses, gold nanorods may be useful, for which ~25% rotated in ATP and >50% in GTP with EF_1 [28].

The speed of unloaded rotation monitored with the 40-nm gold beads, as well as the torque that determines the saturating rotary speed of the 0.29-μm bead duplexes, are not affected by SDS at 0.003%. For the fully active F_1 molecules scored in the rotation assays, SDS exerts little effect. The SDS stimulation of the hydrolysis activity in the initial stage, where the enzyme may be considered to be fully active, is apparently inconsistent with the rotation results. However, the initial hydrolysis activity in the bulk assay has always been somewhat lower than the expected value of three times the revolution rate [8]. Presumably, part of TF_1 in our preparation is always inactive from the beginning, in spite of the removal of the tightly bound nucleotides, or that the nucleotide-free TF_1 tends to be quickly inhibited when first exposed to ATP. SDS likely brings this inactive or inhibited fraction into an active form. The SDS-induced increase in the rate of 0.29-μm bead rotation at low [ATP]s where ATP binding is apparently rate limiting (Figs. 5A and 6) also calls for an explanation: it appears as if SDS shortens the ATP-waiting dwells at every 120° (Fig. 6). It is possible that SDS facilitates ATP binding, but we note that the average rotary speeds of the stepping rotation in the presence of 0.003% SDS is close to the average speeds reported by 40-nm gold beads in the absence of SDS [8]. The 40-nm beads stepped ~50% more frequently than micron-long actin filaments on F_1 [8], indicating that friction or obstruction against a micron-sized probe increases the ATP-binding dwell slightly. SDS likely reduces this impeding factor(s).

Precisely how SDS works on F_1 is not known yet. It seems that SDS does not enhance the intrinsic activity of F_1. Likely, SDS works as a kind of general relaxer or lubricant, removing or lessening a stumbling or impeding factor(s) that is either intrinsic (such as the MgADP inhibition caused by tight binding of MgADP, or possibly internal friction between the subunits of F_1), or extrinsic (such as the friction between the bead and the glass surface or between the bead and F_1).

Acknowledgements

We thank N. Sakaki, R. Shimo-Kon, K. Shiroguchi, T. Okamoto and M. Shio for technical assistance and discussion, and K. Sakamaki and M. Fukatsu for encouragement and lab management. This work was supported by Grants-in-Aid for Specially Promoted Research and the 21st Century COE Program from the Ministry of Education, Culture, Sports, Science and Technology of Japan. M.D. Hossain was supported by the Postdoctoral Fellowship for Foreign Researchers from Japan Society for the Promotion of Science.

References

[1] P.D. Boyer, The binding change mechanism for ATP synthase—some probabilities and possibilities, Biochim. Biophys. Acta 1140 (1993) 215–250.
[2] K. Kinosita Jr., R. Yasuda, H. Noji, K. Adachi, A rotary molecular motor that can work at near 100% efficiency, Philos. Trans. R. Soc. Lond. B. Biol. Sci. 355 (2000) 473–489.
[3] K. Kinosita Jr., K. Adachi, H. Itoh, Rotation of F_1-ATPase: how an ATP-driven molecular machine may work, Annu. Rev. Biophys. Biomol. Struct. 33 (2004) 245–268.
[4] M. Yoshida, E. Muneyuki, T. Hisabori, ATP synthase—a marvellous rotary engine of the cell, Nat. Rev. Mol. Cell Biol. 2 (2001) 669–677.
[5] P.D. Boyer, W.E. Kohlbrenner, The present status of the binding-change mechanism and its relation to ATP formation by chloroplasts, in: B.R. Selman, S. Selman-Reimer (Eds.), Energy Coupling in Photosynthesis, Elsevier, Amsterdam, The Netherlands, 1981, pp. 231–240.
[6] F. Oosawa, S. Hayashi, The loose coupling mechanism in molecular machines of living cells, Adv. Biophys. 22 (1986) 151–183.
[7] J.P. Abrahams, A.G.W. Leslie, R. Lutter, J.E. Walker, Structure at 2.8 Å resolution of F_1-ATPase from bovine heart mitochondria, Nature 370 (1994) 621–628.
[8] R. Yasuda, H. Noji, M. Yoshida, K. Kinosita Jr., H. Itoh, Resolution of distinct rotational substeps by submillisecond kinetic analysis of F_1-ATPase, Nature 410 (2001) 898–904.
[9] K. Shimabukuro, R. Yasuda, E. Muneyuki, K.Y. Hara, K. Kinosita Jr., M. Yoshida, Catalysis and rotation of F_1 motor: cleavage of ATP at the catalytic site occurs in 1 ms before 40° substep rotation, Proc. Natl. Acad. Sci. U. S. A. 100 (2003) 14731–14736.
[10] T. Nishizaka, K. Oiwa, H. Noji, S. Kimura, E. Muneyuki, M. Yoshida, K. Kinosita Jr., Chemomechanical coupling in F_1-ATPase revealed by simultaneous observation of nucleotide kinetics and rotation, Nat. Struct. Mol. Biol. 11 (2004) 142–148.
[11] K. Adachi, K. Oiwa, T. Nishizaka, S. Furuike, H. Noji, H. Itoh, M. Yoshida, K. Kinosita Jr., Coupling of rotation and catalysis in F_1-ATPase revealed by single molecule imaging and manipulation, Cell 130 (2007) 309–321.
[12] H. Itoh, A. Takahashi, K. Adachi, H. Noji, R. Yasuda, M. Yoshida, K. Kinosita Jr., Mechanically driven ATP synthesis by F_1-ATPase, Nature 427 (2004) 465–468.
[13] Y. Rondelez, G. Tresset, T. Nakashima, Y. Kato-Yamada, H. Fujita, S. Takeuchi, H. Noji, Highly coupled ATP synthesis by F_1-ATPase single molecules, Nature 433 (2005) 773–777.
[14] S.R. Paik, J.-M. Jault, W.S. Allison, Inhibition and inactivation of the F_1 adenosinetriphosphatase from *Bacillus* PS3 by dequalinium and activation of the enzyme by lauryl dimethylamine oxide, Biochemistry 33 (1994) 126–133.
[15] J.-M. Jault, T. Matsui, F.M. Jault, C. Kaibara, E. Muneyuki, M. Yoshida, Y. Kagawa, W. S. Allison, The $\alpha_3\beta_3\gamma$ complex of the F_1-ATPase from thermophilic *Bacillus* PS3 containing the $\alpha D_{261}N$ substitution fails to dissociate inhibitory MgADP from a catalytic site when ATP binds to noncatalytic sites, Biochemistry 34 (1995) 16412–16418.
[16] J.-M. Jault, C. Dou, N.B. Grodsky, T. Matsui, M. Yoshida, W.S. Allison, The $\alpha_3\beta_3\gamma$ subcomplex of the F_1-ATPase from the thermophilic *Bacillus* PS3 with the βT165S substitution does not entrap inhibitory MgADP in a catalytic site during turnover, J. Biol. Chem. 271 (1996) 28818–28824.
[17] M.J. Datiles, E.A. Johnson, R.E. McCarty, Inhibition of the ATPase activity of the catalytic portion of ATP synthases by cationic amphiphiles, Biochim. Biophys. Acta 1777 (2008) 362–368.
[18] A. Tanaka, E. Hoshino, Thermodynamic and activation parameters for the hydrolysis of amylose with *Bacillus* α-amylases in a diluted anionic surfactant solution, J. Biosci. Bioeng. 93 (2002) 485–490.
[19] T. Shibatani, W.F. Ward, Sodium dodecyl sulfate (SDS) activation of the 20S proteasome in rat liver, Arch. Biochem. Biophys. 321 (1995) 160–166.
[20] J.E. Mogensen, P. Sehgal, D.E. Otzen, Activation, inhibition, and destabilization of *Thermomyces lanuginosus* lipase by detergents, Biochemistry 44 (2005) 1719–1730.
[21] K. Adachi, H. Noji, K. Kinosita Jr., Single molecule imaging of the rotation of F_1-ATPase, Methods Enzymol. 361B (2003) 211–227.
[22] M.D. Hossain, S. Furuike, Y. Maki, K. Adachi, M.Y. Ali, M. Huq, H. Itoh, M. Yoshida, K. Kinosita Jr., The rotor tip inside a bearing of a thermophilic F_1-ATPase is dispensable for torque generation, Biophys. J. 90 (2006) 4195–4203.
[23] N. Sakaki, R. Shimo-Kon, K. Adachi, H. Itoh, S. Furuike, E. Muneyuki, M. Yoshida, K. Kinosita Jr., One rotary mechanism for F_1-ATPase over ATP concentrations from millimolar down to nanomolar, Biophys. J. 88 (2005) 2047–2056.
[24] T. Matsui, E. Muneyuki, M. Honda, W.S. Allison, C. Dou, M. Yoshida, Catalytic activity of the $\alpha_3\beta_3\gamma$ complex of F_1-ATPase without noncatalytic nucleotide binding site, J. Biol. Chem. 272 (1997) 8215–8221.
[25] Y. Hirono-Hara, H. Noji, M. Nishiura, E. Muneyuki, K.Y. Hara, R. Yasuda, K. Kinosita Jr., M. Yoshida, Pause and rotation of F_1-ATPase during catalysis, Proc. Natl. Acad. Sci. U. S. A. 98 (2001) 13649–13654.
[26] J.-M. Jault, W.S. Allison, Slow binding of ATP to noncatalytic nucleotide binding sites which accelerates catalysis is responsible for apparent negative cooperativity exhibited by the bovine mitochondrial F_1-ATPase, J. Biol. Chem. 268 (1993) 1558–1566.
[27] N.J. Turro, X.-G. Lei, K.P. Ananthapadmanabhan, M. Aronson, Spectroscopic probe analysis of protein-surfactant interactions: the BSA/SDS system, Langmuir 11 (1995) 2525–2533.
[28] J. York, D. Spetzler, T. Hornung, R. Ishmukhametov, J. Martin, W.D. Frasch, Abundance of *Escherichia coli* F_1-ATPase molecules observed to rotate via single-molecule microscopy with gold nanorod probes, J. Bioenerg. Biomembr. 39 (2007) 435–439.